^{18}O Isotope Concentration Control

Valentin Sita[1], Vlad Mureşan[1], Mihail Abrudean[1], Mihaela-Ligia Ungureşan[2] and Iulia Clitan[1]
[1]*Automation Department, Technical University of Cluj-Napoca, Memorandumului street, no. 28, Cluj-Napoca, Romania*
[2]*Department of Physics and Chemistry, Technical University of Cluj-Napoca, Memorandumului street, no. 28, Cluj-Napoca, Romania*

Keywords: ^{18}O Isotope, Concentration Control, Mathematical Model, Neural Network, Distributed Parameter Process, Nonlinear System, Independent Variable.

Abstract: The paper presents a solution to control the ^{18}O isotope concentration at the output of a separation column. The proposed mathematical model which describes the work of the separation column is a distributed parameter one and it approximates with high accuracy the work of the real plant. The isotope separation process is included in a complex control structure which generates high control performances. In order to improve significantly the separation column productivity, an original solution for the efficient rejection of the disturbances effects, is proposed. Also, a solution to determine the instantaneous value of the separation column length constant is proposed, solution which opens the possibility to implement new control strategies.

1 INTRODUCTION

The separation column for the ^{18}O isotope and the equipment of the refluxing system necessary for its work is presented in Fig. 1. In this context, the ^{18}O isotope separation is made through isotopic exchange in the system NO, NO_2-H_2O, HNO_3 (Abrudean, 1981). In Fig. 1, FSC is the Final Separation Column, the term "Final" being used due to the fact that this column works as the final column of a separation cascade which contains two separation columns. The main aim of this paper is to control the FSC work in the case when it works independently from the separation cascade. The results of this research activity, consisting from the proposed control strategy, will be further used in order to find an appropriate method to control the separation cascade work.

As it can be remarked in Fig. 1, FSC has the height h = 10 m, being built from 5 sectors (S1 – S5), each having the height h/5 = 2 m. The column diameter is d = 14 mm. The separation of the ^{18}O isotope is based on the circulation in FSC, in counter-current, of the nitric oxides (NO, NO_2) introduced in the lower part of the column and of the nitric acid (HNO_3) – solution introduced in the upper part of the column. The input flow of nitric oxides is notated with F_i and the output flow of nitric acid is notated to F_W, representing the isotopic waste of the separation process. F_o represents the output flow of the nitric oxides from FSC which is circulated to the arc-cracking reactor ACR. At the ACR output, the flow F_N of both nitrogen (N_2) and nitric oxides (NO, NO_2) results, with an increased concentration of NO_2. In the absorber A, the absorption of the nitric oxides in water is made, resulting nitric acid solution which supplies FSC (the flow of nitric acid solution is notated with F_A). The absorber A is supplied with the water flow F_{H2O}. The amount of nitrogen and nitric oxide from the absorber output, under the flow F_{NN} (NO, N_2) is sent to the catalytic reactor CR. In CR, the water with which the absorber is supplied results through the reaction of nitric oxide (NO) with hydrogen (H_2) (CR is supplied with the hydrogen flow F_H). Also, after the reaction from CR, the excess of nitrogen and hydrogen results (the flow F_{NH}).

The product can be extracted from the top of FSC under the form of nitric acid with an increase concentration of ^{18}O isotope ($HN^{18}O_3$). The product flow is notated with F_P and the corresponding pipe is figured with dashed line due to the fact that in this paper, only the total reflux (F_P = 0) working regime is approached. The hachure used in Fig. 1 signifies

Sita, V., Mureşan, V., Abrudean, M., Ungureşan, M-L. and Clitan, I.
^{18}O Isotope Concentration Control.
DOI: 10.5220/0006877403690379
In *Proceedings of the 15th International Conference on Informatics in Control, Automation and Robotics (ICINCO 2018) - Volume 1*, pages 369-379
ISBN: 978-989-758-321-6

the fact that the corresponding elements contain packing (steel packing in the case of FSC and in the case of the reactors) and ceramic packing (Axente, 1984) in the case of the absorber. In order to measure the concentration of the ^{18}O isotope, at the separation column output, a mass spectrometer is used.

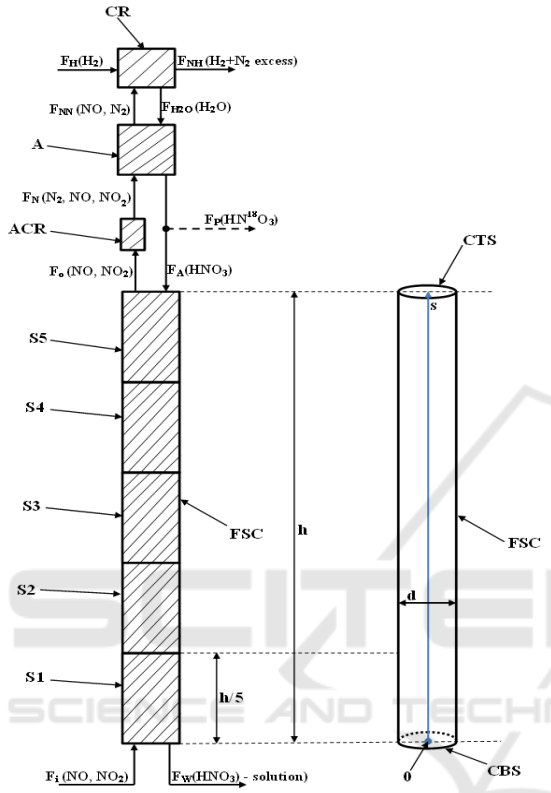

Figure 1: The separation column for the ^{18}O isotope and the equipment of the refluxing system.

2 ISOTOPE SEPARATION PROCESS MODELLING

The ^{18}O isotope separation process is a distributed parameter one (Colosi, 2013; Li, 2011) due to the fact that during the separation exchange, the main output signal (the ^{18}O isotope concentration) depends on two independent variables: time (t) and the position in FSC length (s). In order to highlight the position in FSC length, the (0s) axis is defined (in Fig. 1). The origin (0) of the (0s) axis represents the centre of the Column Base Section (CBS). The independent variable (s) has an increasing evolution from the column base to the column top and its maximum value can be obtained for s = h, corresponding to the Column Top Section (CTS). The main input signal in the process is considered the input flow of nitric oxides $F_i(t)$ and, as it was previously mentioned, the main output signal from the process is considered the ^{18}O isotope concentration notated with y(t,s). The mathematical modelling is made in the hypothesis when FSC works in total reflux regime ($F_P = 0$). This regime is used in the first part of the plant working with the purpose of increasing the ^{18}O isotope concentration until the imposed value, at the column top, is reached. This working regime is the most relevant one for the FSC dynamics.

The mathematical model which describes with high accuracy the work of FSC is proposed in (Mureşan, 2018). This model is briefly presented in the following equations. The final form of the output signal is given by:

$$y(t,s) = y_0 + y_f(t) \cdot \frac{F_{sl}(s) - y_0}{F_{sl}(s = s_f = h) - y_0} = y_0 + y_f(t) \cdot \frac{e^{\frac{s}{S}} - 1}{e^{\frac{s_f}{S}} - 1} \quad (1)$$

where $y_0 = 0.204\%$ represents the natural abundance of the ^{18}O isotope. Also, the $y_f(t)$ function models the separation process dynamics in relation to time (t), representing the solution of the ordinary differential equation:

$$\frac{dy_f(t)}{dt} = -\frac{1}{T(F_i)} \cdot y_f(t) + \frac{1}{T(F_i)} \cdot u_f \quad (2)$$

where $T(F_i)$ is the isotope exchange process time constant which depends on the input flow $F_i(t)$ and $u_f(t)$ represents the increase of the ^{18}O concentration over the y_0 value, in steady state regime. The previously presented differential equation is solved considering the remark that firstly the value of the time constant is singularized for a certain (F_i). The linear variation of the time constant in relation to the input signal ($T(F_i)$) is given by:

$$T(F_i) = T_2 + K_T \cdot (F_i - F_2) \quad (3)$$

where F_2 = 185 l/h (implying the time constant T_2 = 84.703 h experimentally determined) and $K_T = -3.9262 \frac{h^2}{l}$ represents the gradient of the ramp $T(F_i)$. The $u_f(t)$ signal has the following form:

$$u_f = y(t_f, s = s_f = h) - y_0 = y_0 \cdot (S(F_i) - 1) = \\ = y_0 \cdot (\alpha^{n_{tp}(F_i)} - 1) \quad (4)$$

where t = t_f is the final value for time (corresponding to the steady state regime) and s = s_f is the final value for the independent variable (s) (corresponding to the column top). Also, $S(F_i) = \alpha^{n_{tp}(F_i)}$ represents the separation, being a function which depends on the input signal. In its equation, α = 1.018 is the elementary separation factor of the ^{18}O isotope for the isotopic exchange procedure in the system NO, NO_2-H_2O, HNO_3. Also, the equation of the number of the theoretical plates is:

$$n_{tp}(F_i) = \frac{h}{HETP(F_i)} \quad (5)$$

where HETP (F_i) is the Height of Equivalent Theoretical Plate. Both n_{tp} and HETP are functions depending of the input signal (F_i). The HETP variation is linear on intervals, but is nonlinear on the entire domain of F_i values. The HETP function is given by the following system of equations (being linear on intervals, but is nonlinear on the entire domain of F_i values):

$$\begin{cases} HETP(F_i) = HETP_0 + K_{H1} \cdot (F_i - F_0), \text{if } F_i \le 140\,l/h \\ HETP(F_i) = HETP_0 + K_{H2} \cdot (F_i - F_0), \text{if } F_i > 140\,l/h \end{cases} \quad (6)$$

where $HETP_0$ = 8.6 cm obtained for the input flow F_0 = 140 l/h, and K_{H1}, respectively K_{H2} ($K_{H1} = -0.08\ \frac{cm \cdot h}{l}$ for $F_i \le 140\ l/h$; $K_{H2} = 0.0333\ \frac{cm \cdot h}{l}$ for $F_i > 140\ l/h$) are the gradients of the two ramps from (6) (experimentally determined). The HETP (F_i) function is graphically represented in Fig. 2.

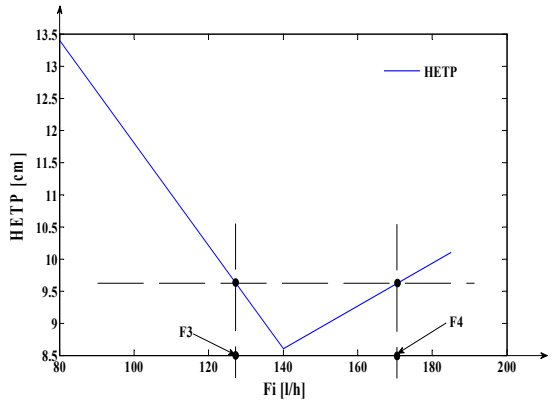

Figure 2: The HETP dependency in relation to F_i.

In order to avoid the usage of the two equations from (6), a neural network is trained to learn the HETP(F_i) function. The structure of the used neural network is a feed-forward fully connected one (Haykin, 2009; Vălean, 1996), having one input signal (F_i), one hidden layer (containing 20 neurons) and one output signal (HETP(F_i)). The neurons of the hidden layer are nonlinear having as activation function the hyperbolic tangent and the output neuron is linear. After training, the neural network output, more exactly the HETP(F_i) function, is given by:

$$HETP(F_i) = WL \cdot \tanh(W \cdot F_i + B) + b_o \quad (7)$$

where WL, W, B and b_o are the training solutions (WL is the row vector which contains the input weights, W is the column vector which contains the layer weights, B is the column vector which contains the bias values of the neurons from the hidden layer and b_o is the output neuron bias value). Also, the notation "tanh" represents the hyperbolic tangent function.

The $F_s(s) = \frac{e^{\frac{s}{S}} - 1}{e^{\frac{s_f}{S}} - 1}$ function from (1) highlights the proportion of the ^{18}O isotope concentration in a certain position from the FSC height, in relation to the ^{18}O isotope concentration at the FSC top. Practically, $F_s(s)$ function models the concentration evolution on the column height. The $F_S(s)$ function is obtained using the $F_{s1}(s) = y_0 \cdot e^{\frac{s}{S}}$ function which approximates the ^{18}O isotope concentration distribution on the FSC height, for a certain (F_i) (implicitly for a certain HETP(F_i)). In the $F_{s1}(s)$ function, (S) represents the "length" constant of the column and depends on the input signal F_i. The S(F_i) function is given by the system of two equations from (8).

$$\begin{cases} S(F_i) = S_1 + K_{S1} \cdot (F_i - F_1), \text{if } F_i \le 140\,l/h \\ S(F_i) = S_2 + K_{S2} \cdot (F_i - F_2), \text{if } F_i > 140\,l/h \end{cases} \quad (8)$$

where S_1 = 751.124 cm obtained for F_1 = 80 l/h and S_2 = 565.5 cm obtained for F_2 = 185 l/h. Also, K_{S1} and K_{S2} ($K_{S1} = -4.4804\ \frac{cm \cdot h}{l}$ for $F_i \le 140\ l/h$; $K_{S2} = 1.8489\ \frac{cm \cdot h}{l}$ for $F_i > 140\ l/h$) are the gradients of the two ramps from (8) (experimentally

determined). From (8), it can be remarked that $S(F_i)$ has an evolution linear on intervals, but nonlinear on the entire domain of F_i values. In order to learn the $S(F_i)$ function, the neural structure as in the case of $HETP(F_i)$ function is used, but having 50 neurons in the hidden layer. After training, the neural network output, more exactly the $S(F_i)$ function, is given by:

$$S(F_i) = WL \cdot \tanh(W \cdot F_i + B) + b_o \quad (9)$$

where WL, W, B and b_o have the same significance as in the case of $HETP(F_i)$ function. Obviously, WL, W, B and b_o are singularized as values for the $S(F_i)$ function, being the solutions of its corresponding neural network training.

3 THE PROPOSED CONTROL STRATEGY

The proposed control structure for the ^{18}O concentration control is presented in Fig. 3. In Fig. 3, SDPP represents the Separation Distributed Parameter Process which has as input signal the flow of nitric oxides $F_i(t)$ and its work depending, also, on the independent variable (s). The output signal from SDPP is the ^{18}O concentration y(t,s), signal which is not yet affected by the disturbance effect. The main disturbance signal modifies directly the value of SDPP outputs signal, having the value $y_d(t)$. Practically, the final value of the ^{18}O concentration (the final output signal) is $y_1(t,s) = y(t,s) + y_d(t)$. DD is the disturbance delay element, modelling the disturbance propagation into the process and y_{d0} is the steady state value of the disturbance. The main disturbance signal in the control system is represented by the product extraction flow (F_P). Even, the product extraction is a usefully procedure, it can be assimilated with a disturbance due to the fact that extracting ($HN^{18}O_3$), with an increased concentration of ^{18}O, from the column, the ^{18}O isotope concentration in the column decreases. The concentration of ^{18}O isotope is measured using the concentration sensor CS which is a mass spectrometer and generates the feedback signal $r_1(t)$. The automation equipment (Golnaraghi, 2009; Love, 2007) from the ^{18}O isotope control system works with unified current signals (4 – 20 mA), obviously $r_1(t)$ being an unified current signal. The actuating signal ($F_i(t)$) is generated by the actuator, in this case the nitric oxides pump P. MSFP represents the reference Model of the System Fixed Part (which includes the mathematical models of the pump P, of SDPP and of the sensor CS, serial connected). It is run on a process computer in parallel with the real process, having its initial (reference) behaviour (not affected by the exogenous disturbances ($y_d(t) = 0$) and not affected by parametric disturbances). The SDPP is integrated in MSFP by implementing the mathematical model presented in Section 2. Also, the mathematical models of P and CS are integrated in MSFP by implementing for each a neural network. The two neural networks have nonlinear autoregressive structure with exogenous inputs (NARX), they contain, each, 9 linear neurons in the hidden layer (they have only one hidden layer) and one linear neuron in the output layer, respectively they have, each, two unit delays (one on the input signal and one on the output signal, due to the fact that P and CS are first order systems).

The main error signal is $e_1(t) = w(t) – r_1(t)$, where w(t) is the concentration setpoint signal. The main concentration controller CC of PID (Proportional – – Integral – Derivative) type, processes the signal $e_1(t)$ and generates the main control signal $c_1(t)$. The secondary error signal $e_2(t) = r_1(t) – r_2(t)$, where $r_2(t)$ is the feedback signal generated at the output of MSFP, represents the measure of the effects of all disturbances (both exogenous and of parametric type) which occur in the system. Practically, $e_2(t)$ is a measure of the deviation of the output signal value in relation to its reference value (generated by the simulation of MSFP). For a correct comparison between the real plant behaviour (referring to the fixed part) and its reference model behaviour, at the input of both entities, the same input signal $c_f(t)$ is applied. The mentioned parametric disturbances can be of two types: the small variations in relation to time of the separation column structure parameters or the small variations of (s) independent variable (due to the change of the CS position and of the product extraction point; due to this aspect, the reference model is simulated for $s = s_f$). The disturbances compensator DC of PD type (Proportional – Derivative) processes the error signal $e_2(t)$ and generates the compensation control signal $c_2(t)$. The total control signal due to the control efforts of CC and DC results as $c_3(t) = c_1(t) – c_2(t)$. The final control signal $c_f(t)$ results as $c_f(t) = c_0 – c_3(t)$, where c_0 represents the value, in unified current, proportional with the value of the reference flow. The reference flow is referring to the initial flow at which the separation column starts to work.

From (3), the fact the lowest value of the separation column time constant is obtained for the flow F_2.

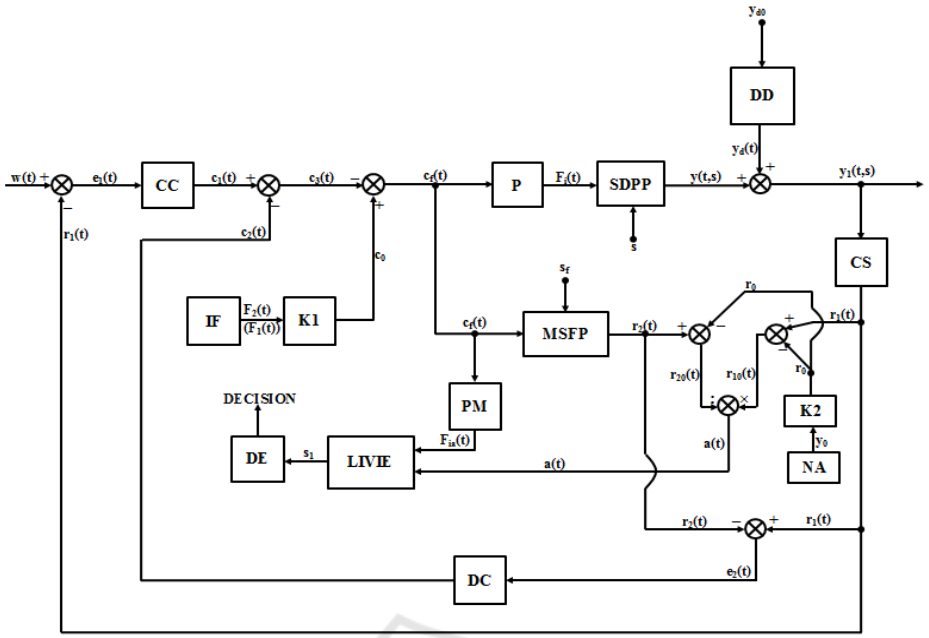

Figure 3: The proposed control structure.

Consequently, in order to obtain an acceptable value of the concentration control system settling time, the reference flow is fixed at the value of F_2. Also, other values could be chosen for the reference flow (for example F_1) but we would obtain a slower control system. The element IF (Initial Flow) generates the value F_2 which is scaled to the c_0 value using the proportionality constant K1.

The instantaneous value of (s) independent variable is determined using LIVIE (Length Independent Variable Identification Element), more exactly the sensor position in the column. This procedure is necessary in order to determine if the separation plant can be physically used when the sensor position in the column is changed. Another advantage of this procedure is the possibility to equivalate the disturbances effects with the change of the CS position in the column. The work of LIVIE is based on obtaining the $F_S(s)$ function from the ratio between the feedback signals $r_{10}(t)$ and $r_{20}(t)$, resulting the signal a(t) ($a(t)=\frac{r_{10}(t)}{r_{20}(t)}$). The feedback signals $r_{10}(t)$ and $r_{20}(t)$ result as differences between the primary feedback signals $r_1(t)$, respectively $r_2(t)$ and r_0, which is the value in unified signal corresponding to the ^{18}O natural abundance (y_0). The value of (y_0) is generated by NA (Natural Abundance Element), after that it being scaled with the proportionality constant K2, resulting (r_0). Obviously, at the plant work starting, $r_{20}(t)$ is initialized at a value different than 0, in order to make possible the computation of a(t). The instantaneous value of the independent variable (s), notated with (s_1), can be obtained from the equation of $F_S(s)$, being given by:

$$s_1 = S(F_i(t)) \cdot \ln[a(t) \cdot e^{\frac{sf}{S(F_i(t))}} + (1-a)] \quad (10)$$

The numerical implementation of (10) is made by LIVIE. The two input signals in LIVIE are a(t) and $F_{ia}(t)$ which is the approximated value of the actuating signal $F_i(t)$. The signal $F_{ia}(t)$ is generated by the simulation of PM (Pump Model) element, which is implemented using the same procedure as in the case of MSFP and having as input signal the $c_f(t)$ signal. The natural logarithm and the exponential function from (10) are numerically implemented using feed-forward fully connected neural networks, too. The Decision Element (DE) generates the "DECISION" in relation to the identified value of (s_1). The "DECISION" can be the generation of an alarm if the (s_1) variable tends to reach the limit value or the separation plant stop if (s_1) variable equals the imposed limit.

In case of the real separation plant, the following elements from Fig. 3: CC, DC, MSFP, LIVIE, PM, IF, K1, NA and K2 have to be implemented on numerical equipment. In order not to increase Fig. 3 complexity in a non-understandable manner, the analog to digital and the digital to analog converters

which connect the numerical equipment to the separation plant are not figured.

4 CONTROLLERS TUNING AND SIMULATIONS RESULTS

The simulations presented in this paper are made in MATLAB/Simulink. The CC tuning is made not considering the disturbances action in the system ($y_{d0} = 0$ and $s = s_f$) and, also, not considering the DC control action ($c_2(t) = 0$). Due to the fact that the isotope separation process, besides being a distributed parameter process, is a strong nonlinear one, the relay method is used for CC tuning. In order to obtain an oscillatory variation of the output signal y(t,s), the CC controller is replaced with a two position relay having the output commutation between the value $b_{min} = 0$ mA and the value $b_{max} = 6.4$ mA (without considering the initial value of 4 mA for the unified current signals), respectively having the hysteresis set to ±1 mA.

If the simulation is made for a step type setpoint signal (proportional with the imposed value of 1.5 % for the output ^{18}O isotope concentration), the control system response (the variation in relation to time of the y(t,s) signal) is presented in Fig. 4.

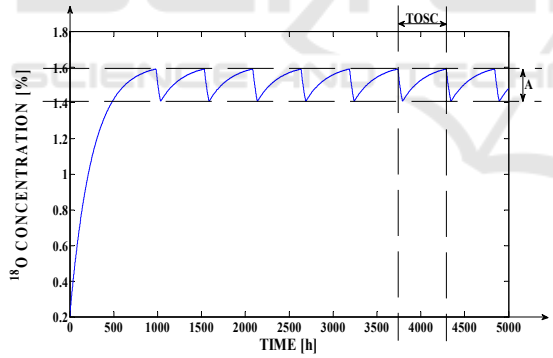

Figure 4: The control system response in the case of the relay tuning method application.

In Fig. 4, the fact that the constant amplitude oscillations are obtained, after 1000 h from the simulation start, is highlighted. From Fig. 4, the oscillation period $T_{OSC} = 552$ h and the oscillation amplitude $A_{OSC} = A/2 = 0.0907$ % result. Using the values obtained for T_{OSC} and A_{OSC}, the parameters of the PID CC controller can be computed using the Ziegler – Nichols equations. The PID controller transfer function is:

$$H_{CC}(s) = K_{CC} \cdot (1 + \frac{1}{T_{ICC} \cdot s} + \frac{T_{DCC} \cdot s}{T_{fCC} \cdot s + 1}) \quad (11)$$

where K_{CC} is the controller proportionality constant, T_{ICC} is the controller integral time constant, T_{DCC} is the controller derivative time constant and T_{fCC} is the time constant of the first order filter used to make the PID controller feasible. After the application of Ziegler – Nichols equations, the fine tuning of the controller is made in order to obtain better control performances. The fine tuning consists in modifying the initial form of the obtained controller parameters and in testing the control performances variation, until the best set of performances is obtained. At the tuning procedure end, the following parameters are obtained: $K_{CC} = 0.358$, $T_{ICC} = 197.143$ h, $T_{DCC} = 33.12$ h and $T_{fCC} = 0.625$ h. If the setpoint concentration is set to 1.5%, the comparative graph between the separation process open loop response and the control system responses for the cases of using the best PI controller that could be obtained respectively using the proposed PID controller, is presented in Fig. 5. In Fig. 5, the notation CSt signifies the minimum concentration value of the steady state band near the steady state value of the output signal (the steady state band is fixed at ±2%, more exactly CSt = 1.47 %).

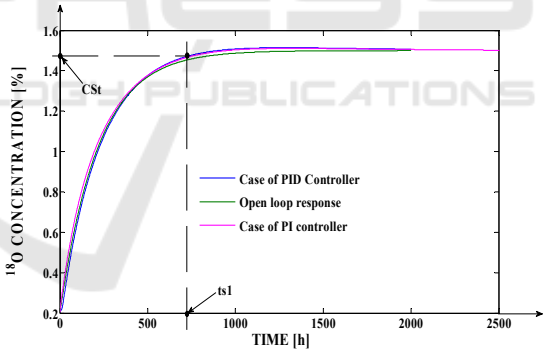

Figure 5: The comparative graph between the open loop separation process response and the control system responses using two different controllers.

From Fig. 5, it results that in all three simulation cases, the steady state error $e_{st} = 0$ %, due to the fact that, in steady state regime the three curves reach the imposed value for ^{18}O concentration ($y_{st} = 1.5$ %). Also, in the case of using both controllers, a small overshoot occurs, having the value smaller than 1 % (the maximum imposed limit). The PID controller generates the overshoot $\sigma_1 = 0.94$ %, insignificantly higher than $\sigma_2 = 0.9$ % (generated by the PI controller). Obviously in the case of the separation process open loop response the overshoot

is σ_3 = 0 %. Due to the fact that in all three cases the overshoot is included in the steady state band, the settling time (which is a critical performance) is considered when the curves from Fig. 5 reach the CSt value. In Fig. 5, the fact that the PID controller generates the smallest settling time t_{s1}, results. In order to distinguish the three values of the settling times, Fig. 6 is considered.

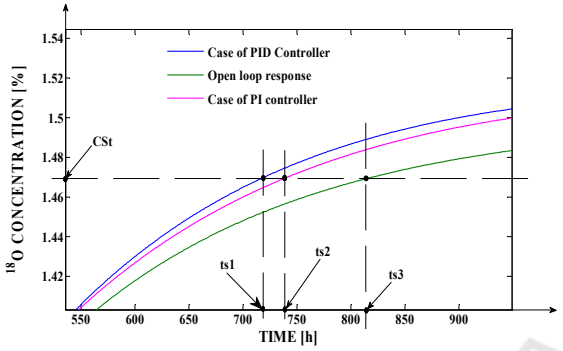

Figure 6: The settling times associated to the three curves from Fig. 5.

From Fig. 6, the fact that the PID controller generates the best settling time (t_{s1} = 719.58 h) is highlighted. It can be remarked that $t_{s1} < t_{s2} < t_{s3}$ (t_{s2} = 740.21 h and t_{s3} = 819.92 h). Consequently, the PID controller usage, improves significantly the separation plant settling time implying important economic advantages. Also, using the PID controller, even better settling times were obtained in simulations, but only if the actuating signal exits from allowed variations limits. Practically, t_{s1} represents the best settling time that could be obtained if the actuating signal ($F_i(t)$) remains enclosed between the saturation limits. The open loop separation process simulation is made simulating the mathematical model presented in Section II for the input flow F_5 = 150.255 l/h, value which generates the steady state value of 1.5 % for the output ^{18}O concentration (according to (3) and (6), the best settling time for the open loop process, if we impose a certain value of the output signal, is obtained if $F_i(t) > 140$ l/h). The main problem in the case of usage the separation process in open loop is the fact that the effect of the disturbances cannot be rejected, aspect highlighted in Fig. 7. The simulations from Fig. 7 are made in the same conditions as the simulations from Fig. 5, but the exogenous disturbance with the value $y_{d0} = -0.1$ % occurs in the system at the moment t_1 = 2500 h. The y_{d0} value is propagated in the system through the DD element having the transfer function $H_{DD}(s) = \frac{1}{T_{DD} \cdot s + 1}$, where the time constant T_{DD} = 50 h. Also, the negative value of y_{d0} is physically interpreted as the output ^{18}O isotope concentration decrease, due to the exogenous disturbance effect. From Fig. 7, it results that in the case of the PID controller usage, the disturbance effect is rejected, in steady state regime the system response reaching again the imposed value (y_{st} = 1.5 %).

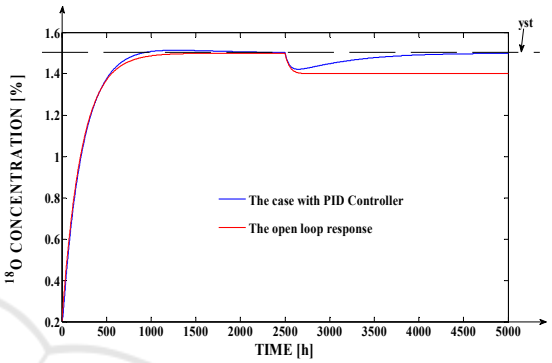

Figure 7: The exogenous disturbance effect.

The open loop response of the separation process, after the disturbance occurs in the system, gets steady to the value y_{st1} = 1.4 % (with y_{d0} smaller than y_{st}, resulting that the disturbance effect is not rejected) fact which highlights again the necessity of using a controller for the concentration control. An important problem which results from Fig. 7 is the slow reaction of the control system in disturbance rejecting regime (the duration of the transitory regime implied by the disturbance effect is over 800 h). In this context, the necessity of using the DC element occurs. For the structure of the Disturbance Compensator (DC) a PD transfer function is proposed, it having the form:

$$H_{DC}(s) = K_{DC} \cdot \frac{T_{DDC} \cdot s + 1}{T_{fDC} \cdot s + 1} \quad (12)$$

The tuning procedure of DC follows the stages: firstly the proportionality constant of DC is initialized at the value K_{DC} = 1, its derivative time constant is initialized at the value T_{DDC} = 10 h, respectively the time constant of the first order filter used to obtain the feasible form of DC is fixed at the value T_{fDC} = 1 h; secondly, T_{DDC} is iteratively determined by increasing its value from an iteration to the next one with ΔT_{DDC} = 1 h until the system response overshoot in disturbance effect rejecting regime occurs (the overshoot values are determined

repeating the simulation at each iteration); finally, K_{DC} is iteratively determined by increasing its value from an iteration to the next one with $\Delta K_{DC} = 0.01$ until the system response overshoot in disturbance effect rejecting regime equals the system response overshoot in starting regime (σ_1). After the application of the presented algorithm, the structure parameters of DC result: $K_{DC} = 1.1$, $T_{DDC} = 50$ h. The comparative graph between the system response in the case of using and the case of not using the DC element, is presented in Fig. 8.

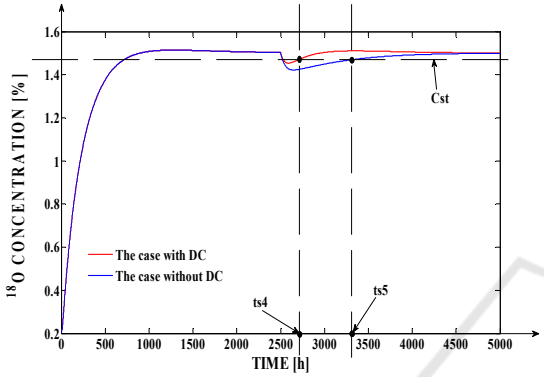

Figure 8: The effect of using DC.

The simulations from Fig. 8 are made in the same conditions as the simulations from Fig. 7. From Fig. 8, it results that the control system generates much better performances in disturbance rejecting regime in the case of using DC than in the case without DC. Relative to the moment t_1 (when the disturbance signal occurs in the system), in the case of using DC, the ^{18}O concentration reaches again the steady state regime after 219.4 h (corresponding to the moment t_{s4}). This transitory regime is much shorter than in the context of not using DC (in this case the ^{18}O concentration reaches again the steady state regime after 842.7 h (corresponding to the moment t_{s5})). Consequently, the usage of DC implies a consistent improvement of the system performances in rejecting the disturbances effects, fact which represents a major technological and economical advantage. The control effort is highlighted in Fig. 9.

From Fig. 9, it results that the variation of the input flow of nitric oxides is enclosed only between the saturation limits [F_1,F_2], aspect which proves that the usage of the two controllers (CC and DC) is feasible. Also, in disturbance effect rejecting regime, due to the action of DC, the actuating signal has a much faster variation, fact which signifies a much stronger control effect and implicitly a higher efficiency of the control system.

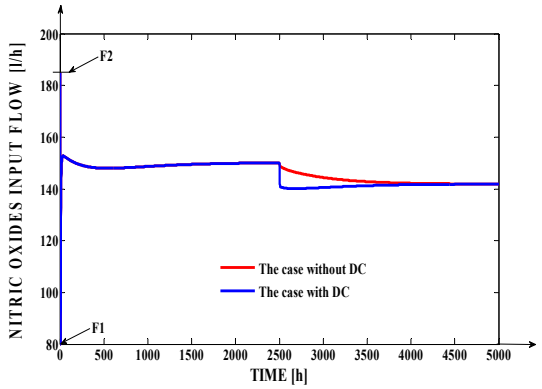

Figure 9: The variation, in relation to time, of the actuating signal.

In Fig. 10, the evolution in relation to time of HETP(F_i) function is presented. This evolution is associated to the system response presented in Fig. 8, in the case of using DC.

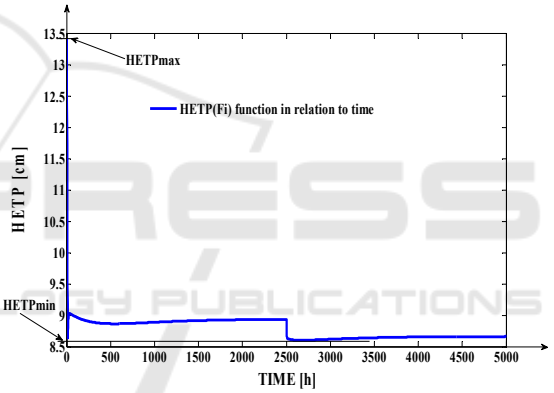

Figure 10: The variation in relation to time of HETP(F_i) function.

From Fig. 10, it results that the limit values of HETP(F_i) presented in Fig.2 ($HETP_{min}$ = 8.6 cm) and ($HETP_{max}$ = 13.4 cm) are almost reached (but not equalled) only in transitory regimes due to the CC, respectively DC actions. This aspect proves again the physical possibility to implement the proposed control strategy. In Fig. 11, the control system response is presented in the case of the (s) independent variable variation. The variation occurs at the moment t_2 = 2500 h from the simulation start, when (s) independent variable value is changed from the initial value s = s_f (s_f = 1000 cm) to the value s = 970 cm. This variation is due to the concentration sensor position change in relation to the column height. In Fig. 11, the fact that the two control elements (CC and DC) reject the effect of the (s) independent variable value "jump", is

highlighted. Only after 237.8 h (corresponding to the moment t_{s6}) from the moment t_2, the ^{18}O concentration equals the CSt value, the imposed steady state regime (near the value y_{st} = 1.5 %) being reached again.

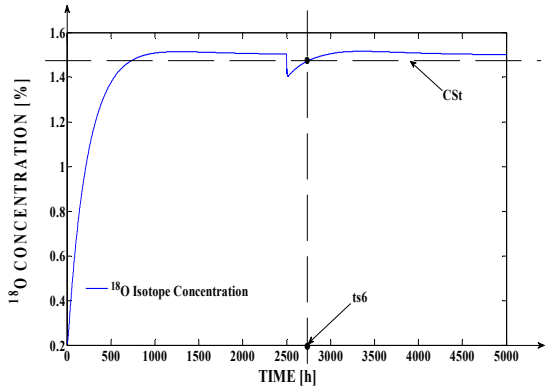

Figure 11: The system response, in the case of the (s) independent variable variation.

This aspect proves the fact that the proposed control structure can efficiently manage the effect of the parametric disturbances, too. The (s) independent variable value change is identified by the LIVIE element. The variation in relation to time of the LIVIE output signal (the approximation (s_1) of the (s) instantaneous value) is presented in Fig. 12.

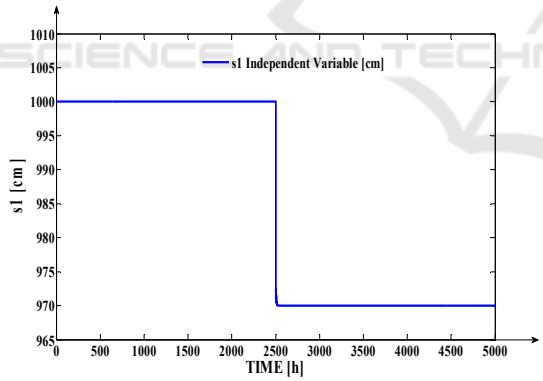

Figure 12: The variation in relation to time of the (s_1) signal.

It can be remarked the fact that the approximation of the (s) independent variable is an exact one both before and after the variation moment (t_2).

In the case when the position of the concentration sensor remains in the position given by s = 970 cm, the ^{18}O isotope concentration evolution, in relation to time, for the value s = s_f, is presented in Fig. 13. From Fig. 13, it results that the ^{18}O isotope concentration increases at the column top (s = s_f). This aspect is explained through the increasing evolution of the output signal in relation to (s) independent variable (according to (1)).

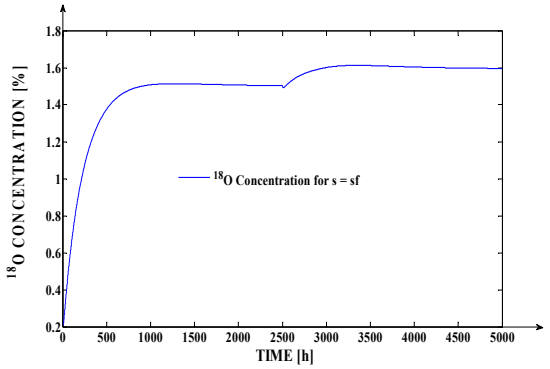

Figure 13: The output signal evolution, in relation to time, for s = s_f.

The change of the concentration sensor position has an important application, more exactly when, immediately after the extraction of the necessary ^{18}O isotope quantity at the imposed concentration (in the example 1.5 %), the isotope extraction at a higher concentration is necessary (for example 1.6 %). In this case, firstly the extraction is made from the point s = 970 cm, where the control is made and secondly, when the ^{18}O isotope concentration has to be increased, the extraction point is changed to s = s_f = 1000 cm (the sensor position can be, also, changed to the column top). The main advantage consists in the avoidance of a new transitory regime and implicitly in a much faster extraction of the ^{18}O isotope at an increased concentration. The procedure of identifying the (s) independent variable value can be, also, used in order to determine if the separation plant can be physically used. The constrain regarding the possibility of usage the separation plant consists in limiting the maximum deviation of the (s) independent variable with more than 40 cm in relation to (s_f) value. In this context, the equivalent value of (s) has to be approximated (containing the superposition of the physical value of (s) and also the equivalent value of (s) (which represents a measure of the exogenous disturbances equated as a position variation in the column height)). In Fig. 14, the same simulation as in the case of Fig. 11 is presented (on the first 5000 h), but considering the fact that at the moment t_3 = 5000 h, an exogenous disturbance with the value y_{d0} = − 0.2 % occurs in the system.

In Fig. 14, the moment t_2 is highlighted with the ellipse 1 and the moment t_3 is highlighted with the ellipse 2. In both cases, the effect of the disturbance

is rejected efficiently, the output signal having in all steady states the imposed value (1.5 %). The evolution, in relation to time, of the signal resulted as the difference ($s_f - s_1$), is presented in Fig. 15.

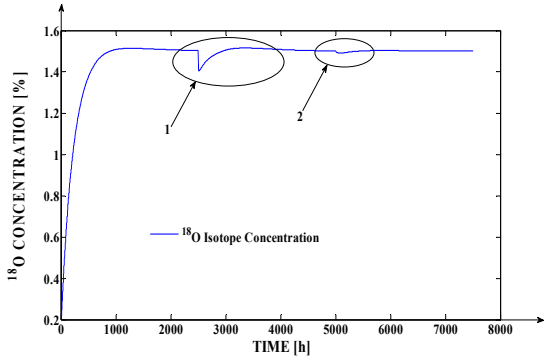

Figure 14: The output signal evolution in relation to time, when both parametric and exogenous disturbances occur in the system.

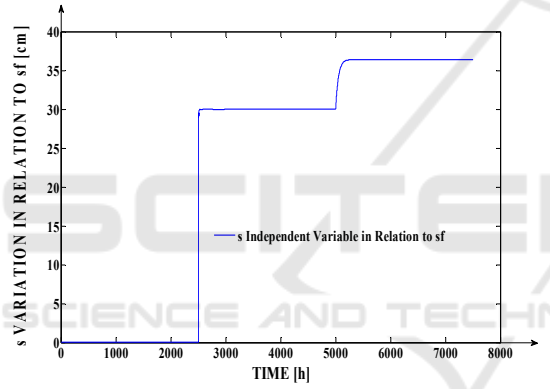

Figure 15: The evolution of (s) independent variable in relation to (s_f).

Practically, the representation from Fig. 15 signifies the equivalent position of the concentration sensor in relation to the column top. After the moment t_3, the value of the signal from Fig. 15 increases with 7 cm (due to the exogenous disturbances). Due to the fact that the maximum value of the signal from Fig. 15 is 37 cm (value smaller than the maximum imposed limit – 40 cm), the conclusion that the system is physically usable at the considered disturbances values, results. At the limit of 40 cm, the effect of the disturbances cannot be rejected without the increase of the actuating signal over the saturation limits. At the detection of the value ($s_f - s = 37$ cm) the DE element from Fig. 3 takes the DECISION of emitting an Alarm and at the detection of the limit value ($s_f - s = 40$ cm), the DE element takes the DECISION of stopping the separation plant. Obviously, the difference ($s_f - s$) is always positive due to the fact that the sensor position can be changed only in the column volume (and only near its top).

5 CONCLUSIONS

In this paper, an original control structure used for the control of the ^{18}O isotope concentration (isotope produced using a separation column), is presented. An important achievement is represented by the fact that the separation process, which is a distributed parameter process, is included in a control system.

In order to obtain high control performances in disturbance rejecting regime, a compensation loop, based on the process reference model, is designed.

The HETP variation in relation to F_i is nonlinear due to the following explanations: at the consistent decrease of F_i, the steel packing of FSC is not properly wet and the contact between the liquid and the gas from the column is not an efficient one, fact which implies a high value of HETP; at the consistent increase of F_i, the formation of the flooding phenomenon occurs, fact which implies a high value of HETP, too; the column optimum HETP (the smallest value of HETP) is obtained in the case of the studied separation column for F_i = 140 l/h which is an intermediary value; each separation column has an optimum point given by its optimum loading.

Considering the previous remarks regarding the HETP value variation, the saturation limits of the actuating signal are determined, obtaining the $[F_1, F_2]$ domain.

Another original element proposed in the paper is the design of an identification system of the exact concentration sensor position in the neighbourhood of the column top. Also, a procedure to equivalate the disturbances effects, with a change of (s) independent variable value, is proposed. These mathematical mechanisms can be used in order to optimize the product extraction from the separation plant, when the future orders (for ^{18}O isotope) can be predicted.

Another application of these mathematical mechanisms is represented by the possibility to determine if the separation plant is physically usable and in the case when it is not, the decision element can take the decision of stopping the plant work.

A future possibility to improve the control system performances is given by the possibility to replace the main CC PID controller with an advanced controller (Kern, 2015; Zou, 2017). Also,

the proposed model can be extended in order to obtain the mathematical model of a separation cascade, which contains two separation columns in its structure. Obviously, for the case of a separation cascade, the proposed control strategy has to be adapted.

REFERENCES

Abrudean, M., 1981. *Ph.D. Thesis*.

Axente, D., Abrudean, M., Bâldea, A., 1994. *^{15}N, ^{18}O, ^{10}B, ^{13}C Isotopes Separation trough Isotopic Exchange*, Science Book House.

Coloşi, T., Abrudean, M., Ungureşan, M.-L., Mureşan, V., 2013. *Numerical Simulation of Distributed Parameter Processes*, Springer.

Golnaraghi, F., Kuo, B. C., 2009. *Automatic Control Systems*, *9th edition*, Wiley Publishing House.

Haykin, S., 2009. *Neural Networks and Learning Machines*, *Third Edition*, Pearson Int. Edition.

Kern, R., Shastri, Y., 2015. Advanced control with parameter estimation of batch transesterification reactor, In *Journal of Process Control*, Vol. 33, pp. 127-139.

Li, H.-X., Qi, C., 2011. *Spatio-Temporal Modeling of Nonlinear Distributed Parameter Systems: A Time/Space Separation Based Approach*, *1st Edition*, Springer.

Love, J., 2007. *Process Automation Handbook*, *1 edition*, Springer.

Mureşan, V., Abrudean, M., Ungureşan, M.-L. Coloşi, T., 2018. Modeling and Simulation of the Isotopic Exchange for 18O Isotope Production, *proposed for publishing to AQTR*, Cluj-Napoca, Romania.

Vălean H., 1996. Neural Network for System Identification and Modelling. In *Proc. of Automatic Control and Testing Conference*, Cluj-Napoca, Romania, 23-24 May, pp. 263-268.

Zou, Z., Wang, Z., Meng, L., Yu, M. Zhao, D., Guo, N., 2017. Modelling and advanced control of a binary batch distillation pilot plant, In *Chinese Automation Congress (CAC)*, 20-22 October.